Am J Transl Res 2019;11(5):3195-3212
www.ajtr.org /ISSN:1943-8141/AJTR0085336

Original Article

Huangqi decoction inhibits hyperglycemia-induced podocyte apoptosis by down-regulated Nox4/p53/Bax signaling *in vitro* and *in vivo*

Zezheng Li[1], Wenjuan Deng[1], Aili Cao[2], Yingjun Zang[1], Yunman Wang[1], Hao Wang[1], Li Wang[2], Wen Peng[1,2]

[1]Department of Nephrology, [2]Laboratory of Renal Disease, Putuo Hospital, Shanghai University of Traditional Chinese Medicine, Shanghai, China

Received September 10, 2018; Accepted March 23, 2019; Epub May 15, 2019; Published May 30, 2019

Abstract: Background: Podocyte dysfunction is associated with the progression of diabetic nephropathy (DN). Huangqi decoction (HQD), a traditional Chinese medical formula, has been used to improve diabetes-related syndrome in China. The present study was to investigate the protective effect of HQD on podocyte apoptosis and the underlying molecular mechanism. Methods: Podocyte was used to measure the efficacy of HQD on cell apoptosis, activities of NADPH oxidases, ROS generation and mitochondrial membrane potential (MMP), and the activation of Nox4/p53/Bax signaling pathway with HQD treatment were also investigated in vitro. Renal pathological morphology, renal function, podocyte apoptosis and Nox4/p53/Bax signaling pathway were investigated with STZ-induced diabetic mice in vivo. Results: HQD increased the cell proliferation and MMP level, while the ROS production and activities of NADPH oxidases were decreased. Meanwhile, Nox4/p53/Bax signaling was down-regulated. Contrarily, overexpression of Nox4 or p53 significantly abolished those efficacies of HQD. Accordingly, in vivo study showed that the progressive albuminuria, glomerulosclerosis and loss of podocytes were significantly alleviated with HQD treatment in diabetic mice, which paralleled by the marked inhibition of Nox4/p53/Bax signaling. Conclusion: Collectively, we provide further evidence that HQD had a renoprotective effect in preventing podocyte apoptosis, which was mediated at least in part by down-regulation of Nox4/p53/Bax signaling.

Keywords: Huangqi decoction, podocytes apoptosis, diabetic nephropathy, oxidative stress, mitochondrial dysfunction, Nox4/p53/Bax signaling

Introduction

Diabetic nephropathy (DN) is one of the most severe diabetes-induced microvascular complications, which leads to end-stage renal disease (ESRD) [1, 2]. As a highly specialized cell type, podocytes are particularly imperative for glomerular filtration barrier, and several recent studies revealed that podocyte depletion may play a crucial role in the progression of DN [3, 4]. Although most evidences have identified that podocyte number and morphology are good predictors for DN development, the potential mechanism remains unclear.

Oxidative stress, characterized by the overgeneration of reactive oxygen species (ROS), which is one of the most risk factors to podocyte apoptosis in DN progression [5, 6]. As the main source of ROS, NADPH oxidase and several NADPH oxidase catalytic subunits such as Nox2, Nox1 and Nox4 are abundantly expressed in kidney [7, 8]. And accumulating evidence have taken Nox4 as the essential target to podocyte injury under high glucose (HG)-induced circumstance [9, 10]. Impairment of Nox4 significantly inhibited NADPH oxidase activity, dramatically reduced caspase-3 activity and HG-induced podocyte apoptosis [11]. Exposed to HG can up-regulate Nox4 and tumor suppressor transcription factor p53 (p53) expression [11]. Then p53 plays a compelling role in apoptotic intrinsic pathway by integrating the action of pro-apoptotic Bax and the action is associated with mitochondrial dysfunction [12, 13]. The mitochondrial apoptotic pathway is initiated by activation of Bax transferring to the outer mitochondrial membrane from cytoplasm, where it

oligomerizes and penetrates the inner mitochondrial membrane [14, 15]. Thus, inhibiting Nox4/p53/Bax signaling may be the reasonable pathway to rescue cell death.

Huangqi decoction (HQD), a classic traditional Chinese medical formula, is composed of seven herbs including *Astragalus (Huang Qi), Poria (Fu Ling), Trichosanthes (Gua Lou), Ophiopogon (Mai Dong), Schisandra (Wu Wei Zi), Licorice (Gan Cao) and Rehmannia (Di Huang).* Our previous studies have revealed that HQD and its active ingredient possessed activities in renal protection, such as inhibiting renal tubulointerstitial fibrosis through TGF-β/Smad and Wnt/β-Catenin signaling pathway [16, 17], ameliorating streptozotocin (STZ)-induced DN through antioxidant mechanism [18] and attenuating endoplasmic reticulum stress-induced podocyte apoptosis [19, 20]. So HQD is considered as a good candidate in preventing DN development, however the underlying mechanism warrants further investigated. In the present study, HG-treated podocyte and STZ-induced diabetic mice was employed to investigate the role of HQD in regulating Nox4/p53/Bax signaling, thus indicting the underlying molecular mechanism to podocytes apoptosis.

Materials and methods

HQD preparation, cell culture and treatment

Astragalus, Poria, Trichosanthes, Ophiopogon, Schisandra, Licorice, and Rehmannia were purchased from Shanghai Huayu Chinese Herbs Co. Ltd. (Shanghai, China). HQD was extracted and the composition of the complete HQD was analyzed by LC-MS as previously reported [21]. Conditionally immortalized mouse podocytes were bountifully provided by Prof. Niansong Wang (Shanghai Sixth People Hospital, China) and cultured in RMPI-1640 supplemented with 10% fetal bovine serum (FBS), 100 U/ml penicillin and 100 mg/ml streptomycin for proliferation. Differentiated podocytes were cultured in RMPI 1640 with 1% FBS for 24 hours before being treated the various experimental conditions. HQD was prepared as previously described [17] and the final concentration in medium was measured by CCK8. Podocytes were seeded at a concentration of 1×10^4 cells/100 μl into 96-well plates for 24 hours. Culture medium was aspirated before HQD in concentration gradient of 0, 10, 30, 100, 300, 1000, 3000, 10000 and 30000 μg/ml were added. After 24 hours, the drug solution was discarded before CCK8 was added and the cultures incubated for 1 hour at 37°C. Absorbance was quantified at 450 nm using a microplate reader. The differentiated podocytes were pretreated with or without HQD and apocynin (100 μM) respectively for 2 hours followed by incubation low D-glucose (5 mM, LG), mannitol (25 mM mannitol + 5 mM D-glucose, M) or high glucose (30 mM, HG) for 72 hours. To confirm whether Nox4 or p53 was involved in the effect of HQD on podocyte apoptosis and regulation of Nox4/p53/Bax signaling, Nox4 or p53 overexpression plasmid for mouse and control vector were transient transfected with Lipofectamine R3000 Reagent (Invitrogen, Carlsbad, CA, USA) for 24 hours before being incubated with 30 mM HG medium with or without HQD and apocynin treatment. Mouse Nox4 and p53 cDNA (GenBank accession NM_015760 and NM_011640) were synthesized respectively and cloned into GV141 vector to create overexpression plasmid, which were synthesized by Genechem Co., Ltd (Shanghai, China). Western blot was performed to confirm the overexpression of Nox4 or p53.

Apoptosis assay by flow cytometry

Podocytes were plated in 6-well plates at the density of 1×10^5 cells per well and cultured under the indicated conditions. Cell apoptosis was performed by FITC Annexin V Apoptosis Detection Kit I (BD Biosciences, Franklin Lakes, NJ, USA) as follows. The mouse podocytes were dissociated using trypsin, washed thrice with PBS and suspended in annexin V binding buffer. Then podocytes were incubated with propidium iodide (PI) in the dark and were analyzed by flow cytometry. Apoptotic podocytes were defined as annexin V-positive/PI-negative (early apoptotic) and annexin V-positive/PI-positive (late apoptotic) cells.

Immunofluorescence staining

Podocytes cultured on coverslips were fixed with 4% paraformaldehyde for 15 minutes, washed thrice with PBS and permeabilized with 0.1% Triton X-100 for 10 minutes. Then cells were blocked with 5% bovine serum albumin (BSA) and 0.1% Triton X-100 for 1 hour at room temperature. Specific primary antibodies including against Nephrin (ab58968, Abcam, MA, USA) and

Nox4 (ab133303, Abcam, MA, USA) were applied overnight at 4°C. After three washes, cells were stained with Cy™ 2 or Cy™ 3-conjugated secondary antibodies (Jackson ImmunoResearch, West Grove, PA, USA) for 1 hour at room temperature. The nuclei were visualized by 4',6-diamidino-2-phenylindole (DAPI) staining. Images were observed with a confocal microscope (LAM880, Zeiss, Germany) or fluorescence microscope (TE2000, Nikon, Japan).

Activity of NADPH oxidases in podocytes

Cultured podocytes were collected after corresponding treatment and podocytes NADPH oxidase activity was evaluated by a lucigenin-enhanced chemiluminescence assay (Nanjing Jiancheng Bioengineering Institute, Nanjing, China) as previously described [7]. Superoxide production was expressed as relative light units/min/mg of protein.

Measurement of ROS generation

The intracellular ROS generation was evaluated using the dihydroethidium (DHE, D-7008, Sigma, USA) fluorescent probe according to the protocol. Pretreated cells were washed with PBS and then continually incubated with DHE probe (10 μM) at 37.0°C for 20 minutes. Cells were washed with PBS to remove free DHE molecules and fixed with 4% paraformaldehyde. Cell images were monitored with a fluorescence microscope (TE2000, Nikon, Japan) and the fluorescence intensity was analyzed at an excitation/emission wavelength of 370/420 nm.

Quantitative RT-PCR (qRT-PCR)

Total RNA and DNA from cultured podocytes were extracted using Trizol reagent (Invitrogen, Carlsbad, CA, USA) and Moloney murine leukemia virus reverse transcriptase (New England Biolabs, Ipswich, MA, USA) according to the instructions of manufacturers. The sequences of the primers were used as previously described [22] and as follows: Nox4, 5'-GAAGGGGTTAAACACCTCTGC-3' (forward primer) and 5'-ATGCTCTGCTTAAACACAATCCT-3' (reverse primer). gp91phox, 5'-TTAGTGGGAGCAGGGATTGG-3' (forward primer) and 5'-CCGGCA TTGTTCCTTTCCT-3' (reverse primer). p22phox, 5'-GCCATTGCCAGTGTGATCT A-3' (forward primer) and 5'-TGGTAGGTGGTTGCTTGATG-3' (reverse primer). p47phox, 5'-GTCCCTGCATCCTATCTGGA-3' (forward primer) and 5'-ATGACCT CAATGGCTTCACC-3' (reverse primer). rac-1, 5'-GCCAATGTTATGGTAGATGGAAA-3' (forward primer) and 5'-TTTCAAATGATGCAGGACTCA-3' (reverse primer). β-actin, 5'-GCGTGACATCAAAGAGAAGC-3' (forward primer) and 5'-CTCGTT GCCAATAGTGATGA-3' (reverse primer). All primers were synthesized by Sangon Biotech Co., Ltd. (Shanghai, China). qRT-PCR was performed in a standard PCR protocol using SuperReal PreMix Plus (SYBR Green) Kit (TIANGEN BIOTECH (BEIJING) CO., LTD; Beijing, China). Cycling conditions were as follows: 10 sec denaturation at 95°C, 31 sec annealing at 58°C for 40 cycles using ViiA7 Standard 96 sequence detection system (Applied biosystems, USA). The relative mRNA amount was determined by relative to the control sample after normalizing to β-actin gene control values and calculated by the comparative cycle threshold ($^{\Delta\Delta}$Ct) method.

Western blot analysis

Podocytes and tissues were collected and lysed in RIPA lysis buffer complemented with protease inhibitor cocktail (Sigma-Aldrich, St Louis, MO, USA) for 30 minutes on ice to acquire total protein. Nuclear proteins were extracted according to the instructions by Cayman (Michigan, MO, USA), and cytosolic and mitochondrial membrane cell fractions were prepared using Cell Mitochondria Isolation Kit (Thermos Fisher scientific, Carlsbad, CA, USA) according to the instructions of manufacturers. The protein concentration was measured by the bicinchoninic acid (BCA) protein assay (Boster Biotechnology, Wuhan, China). Specific primary antibodies used for detection of gp91phox (sc-5827), p47-phox (sc-14015), p22phox (sc-20781) and rac-1 (sc-95) were purchased from Santa Cruz Biotechnology (Santa Cruz, CA, USA); for Nephrin (ab58968), Nox4 (ab133303), p53 (ab131442), p-p53 (ab33889), Histone H1 (ab71580), WT1 (ab89901) and Bcl-xl (ab32370) from Abcam (Cambridge, MA, USA); for β-actin (#4970S), Bcl-2 (#2870), RARP-1 (#9532), caspase 3 (#9665), caspase 9 (#9504s), Bax (#2772), Cytc (#12963S) and β-tubulin (#2146) from Cell Signaling Technology (Danvers, MA, USA). Horseradish peroxidase-conjugated secondary antibodies were purchased from BOSTER (Wuhan, China). Bands were detected by Image Quant LAS 500 imaging system and densitometric quantitation of target proteins were determined

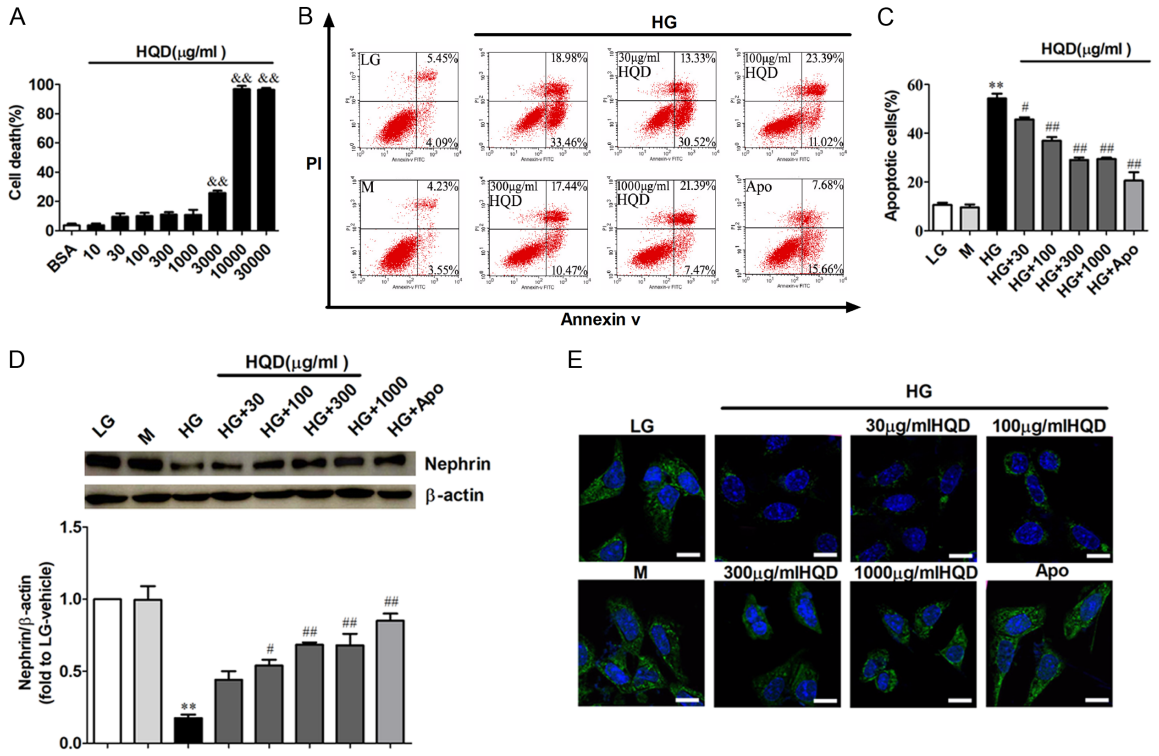

Figure 1. Effect of HQD on HG-induced podocyte apoptosis. (A) Cells were treated with BSA and 0-30000 μg/ml HQD for 24 hours and then cell death was determined by CCK8 assay. $^{\&\&}P < 0.01$, compared with BSA-treated group; (B-E) Podocytes were pretreated with HQD (30, 100, 300, 1000 μg/ml) and apocynin (Apo, 100 μM) for 2 hours followed by high glucose (30 mM, HG) exposure for 72 hours and then subjected to analyses by flow cytometry, western blot and immunofluorescence staining. low D-glucose (5 mM, LG) and mannitol (25 mM mannitol + 5 mM D-glucose, M) were used as controls. (B) Representative flow cytometry pictures and (C) quantitative analysis of apoptotic podocytes under different cultural conditions. (D) Western blot analyses and densitometric quantification of Nephrin expression under different cultural conditions. (E) Immunofluorescence staining for Nephrin under different cultural conditions. Scale bars, 10 μm. One-way ANOVA and Newman-Keuls multiple comparisons test (A, C, D). $^{**}P < 0.01$, compared with LG group; $^{\#}P < 0.05$, $^{\#\#}P < 0.01$, compared with HG group.

by ImageJ software using β-actin, Histone H1 or β-tubulin as the internal control.

Determination of MMP

The integrity of the mitochondrial membrane potential (MMP) in podocytes was measured by flow cytometry using the JC-1 (Thermos Fisher Scientific, Carlsbad, CA, USA). Briefly, treated cells were harvested, washed in ice-cold PBS three times, stained with 2 μM JC-1 at 37°C for 30 min and analyzed by flow cytometry as previous reported [23].

Measurement of mitochondrial superoxide generation

Superoxide production of mitochondria were detected using MitoSOX Red (Thermos Fisher Scientific, Carlsbad, CA, USA) as described previously [24]. Pretreated cells were washed with warm PBS and then continually incubated with the MitoSOX (5 μM) at 37.0°C for 10 minutes avoiding light. Cells were washed gently with PBS to remove free MitoSOX molecules, fixed with 4% paraformaldehyde. Cell images were monitored with a confocal microscope (LAM 880, Zeiss, Germany).

Animal treatment

Male C57BL/6J mice, aged 6 weeks and weighting 16-20 g, were purchased from Shanghai laboratory animal center (Shanghai, China) and raised for 2 weeks of acclimation in a clean conventional environment with a temperature-controlled room under a regular 12/12 hours light/dark cycle and had free access to food and water. All experiments were carried out in accordance with the approved guidelines for

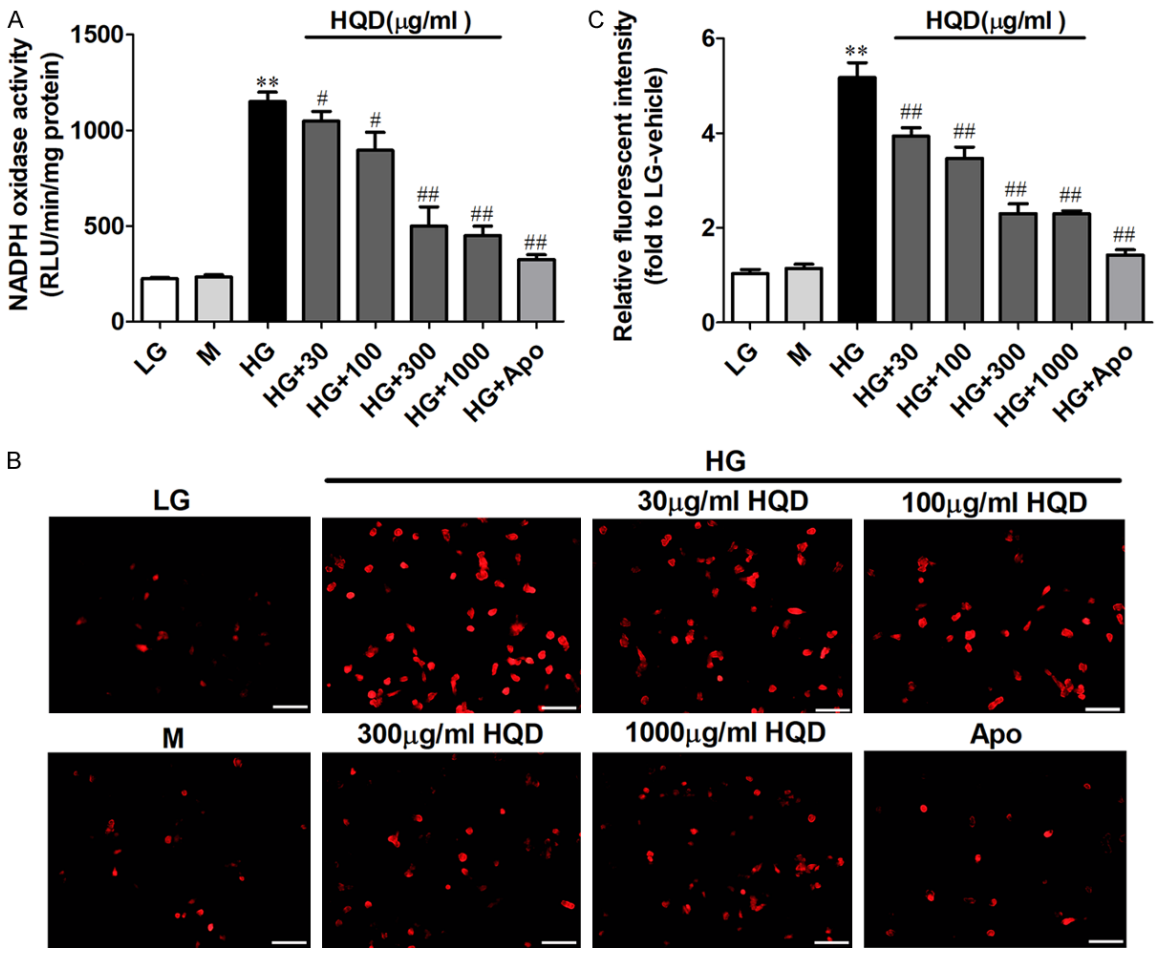

Figure 2. Effect of HQD on NADPH oxidase activity and intracellular ROS generation. Podocytes were pretreated with HQD (30, 100, 300, 1000 μg/ml) for 2 hours followed by HG exposure for 72 hours, then NADPH oxidase activity was analyzed by lucigenin-enhanced chemiluminescence assay (A) and intracellular ROS generation was examined by DHE staining (B). Scale bars, 40 μm. (C) Relative fluorescence intensity of intracellular ROS. One-way ANOVA and Newman-Keuls multiple comparisons test (A, C). $^{**}P < 0.01$, compared with LG group; $^{\#}P < 0.05$, $^{\#\#}P < 0.01$, compared with HG group.

the use and care of experimental animals in Putuo Hospital, Shanghai University of Traditional Chinese Medicine. The animals were induced to diabetes model by intraperitoneal injection of freshly prepared STZ (Sigma-Aldrich, St Louis, MO, USA, dissolved in 0.01 M citrate buffer, pH 4.45) at 100 mg/kg/day for 2 consecutive days. Fasting blood glucose was measured to verify the development of diabetes model 2 weeks after STZ injection. Mice with blood glucose ≥ 16.7 mmol/L were randomly separated into 3 groups (n=8 for each group) and treated respectively with vehicle (0.5% carboxymethyl cellulose), HQD (1.08 g/kg) and apocynin (40 mg/kg) by daily gavage for 8 weeks. Normal control (NC) mice without STZ treatment were randomly divided into 2 groups and administered respectively with vehicle and HQD at 1.08 g/kg as control. The dose of HQD was chosen according to the body surface area normalization method.

Measurement of biochemical parameters

From the 2 weeks after STZ injection, animals were placed into individual metabolic cages every 4 weeks for 24 hours urine collection. At 10 weeks after the start of STZ treatment, blood samples were obtained from the eyeball for serum BUN and creatinine detection, then all mice were killed and kidneys were immediately harvested for protein or for histological analysis. Urinary albumin, BUN and creatinine were tested with commercial ELISA kits (Nanjing

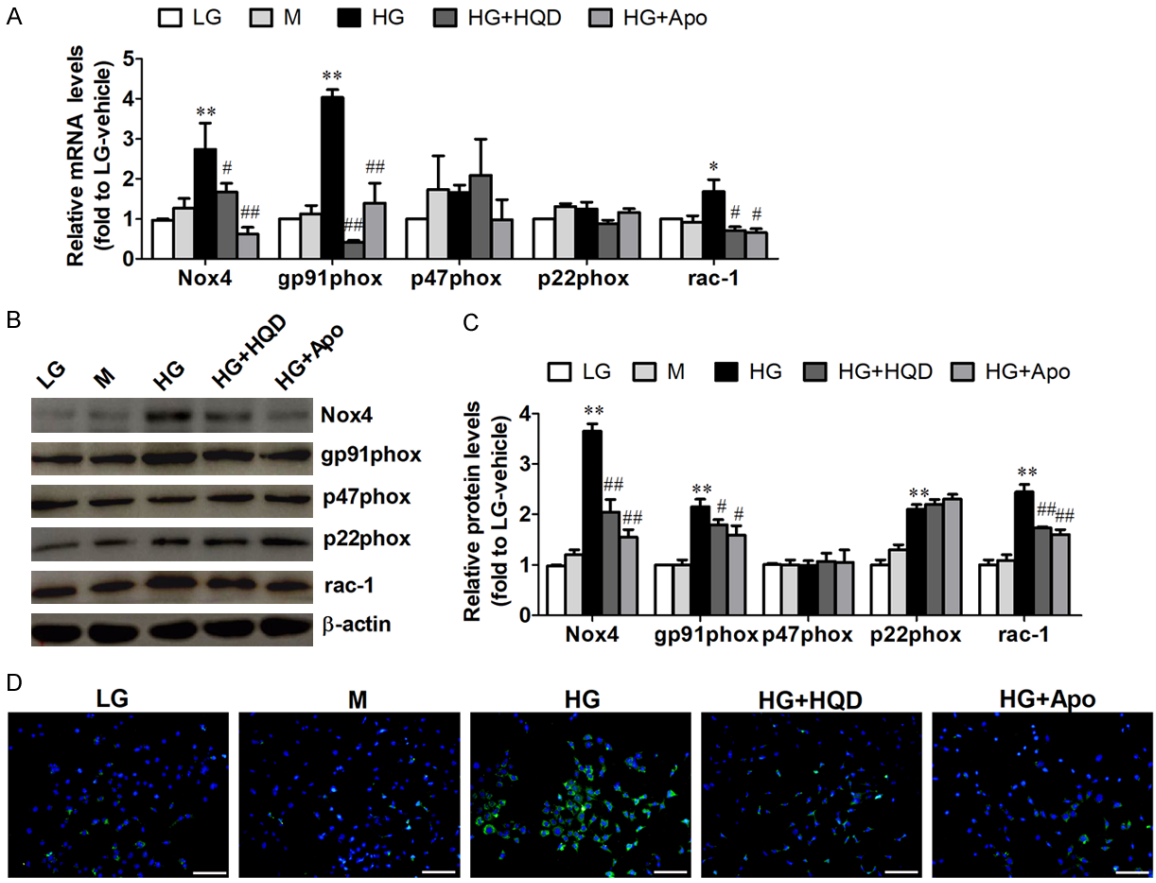

Figure 3. Effects of HQD on NADPH oxidase expression. (A-D) Podocytes were pretreated with HQD (300 μg/ml) for 2 hours followed by HG exposure for 72 hours, then subjected to analyses by qRT-PCR, western blot and immunofluorescence staining. (A) qRT-PCR analysis of NADPH oxidase subunits, including Nox4, gp91phox, p47phox, p22phox and rac-1 mRNA expression. (B) Representative western blot and (C) densitometric quantification of NADPH oxidase subunits expression. (D) Immunofluorescence staining for Nox4 expression. Scale bars, 100 μm. One-way ANOVA and Newman-Keuls multiple comparisons test (A). Unpaired two-tailed t test and Newman-Keuls multiple comparisons test (C). $^{*}P < 0.05$, $^{**}P < 0.01$, compared with LG group; $^{\#}P < 0.05$, $^{\#\#}P < 0.01$, compared with HG group.

Jiancheng Bioengineering Institute, Nanjing, China) and determined according to the instructions of manufacturer.

Renal histology and immunohistochemistry

Renal tissues were fixed in 4% paraformaldehyde (PFA) for 24 hours, dehydrated in gradient, cleared, embedded in paraffin, cut into 4 μm-thick sections and renal sections were stained with periodic acid-Schiff (PAS). Semiquantitative scoring of glomerular sclerosis was performed using a five-grade method. At least 50 glomeruli per section were evaluated by an examiner masked to the experimental conditions. For immunohistochemistry, paraffin-embedded sections were stained with primary antibodies against Nox4 (Abcam, MA, USA) at 4°C overnights for another an hour incubation at 37°C. After incubation with biotinylated secondary antibody (Vector Laboratories, Burlingame, CA, USA), the sections were incubated with VECTASTAIN ABC reagent (Vector Laboratories, Burlingame, CA, USA) and color development was performed using 3, 3' diaminobenzidine (Vector Laboratories, Burlingame, CA, USA).

Statistical analysis

Data are expressed as the means ± SEM. All experiments were repeated a minimum of three times and representative experiments are shown. All statistical analyses were conducted with GraphPad Prism 6.01 (GraphPad Software, La Jolla, CA). Unpaired two-tailed t test or one-way ANOVA followed by the Newman-Keuls mul-

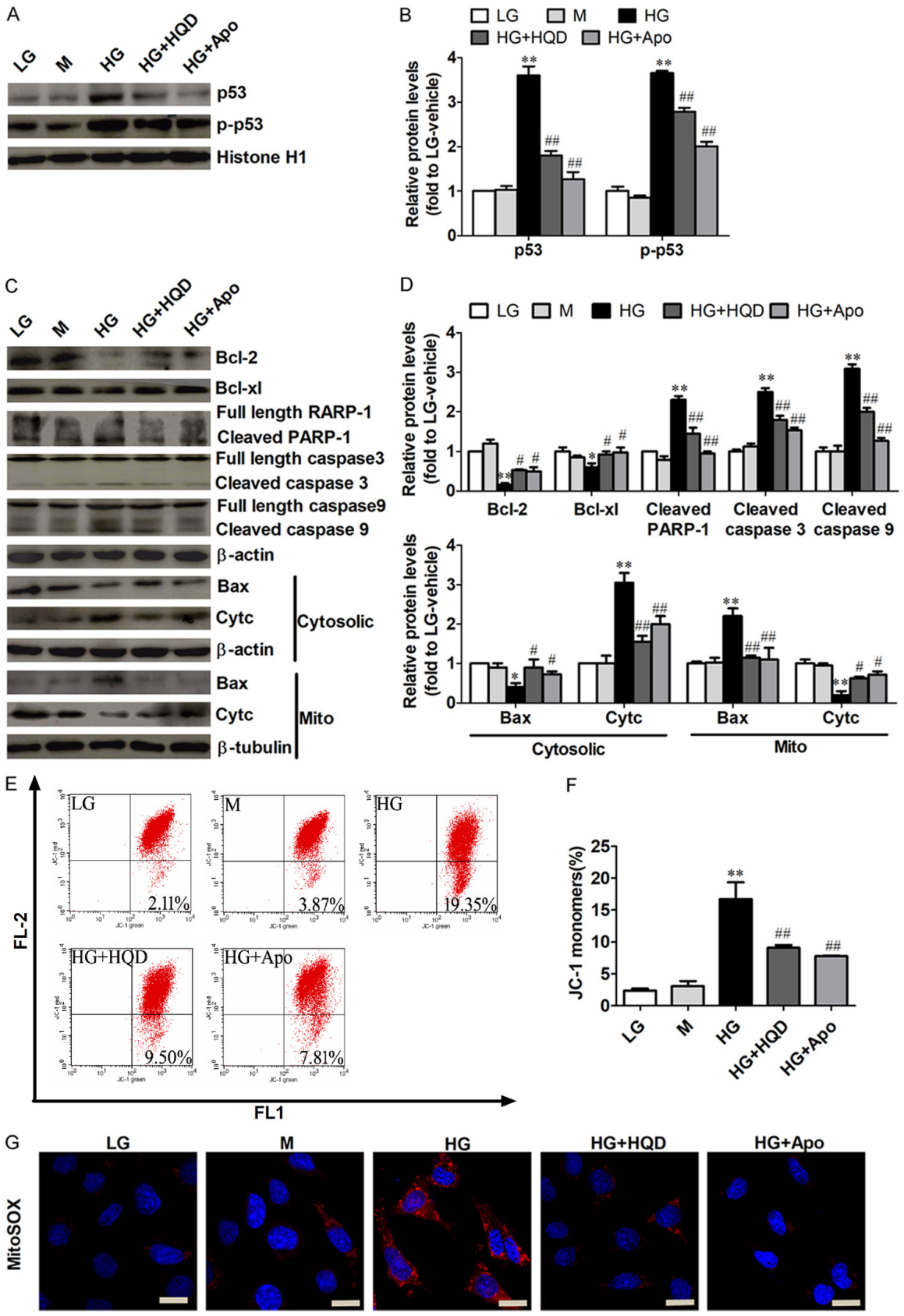

Figure 4. Effect of HQD on Nox4/p53/Bax signaling and mitochondrial-mediated apoptotic pathway in HG-induced podocyte. (A) Representative western blot and (B) densitometric quantification of nuclear p53 and p-p53 expres-

sion. (C) Representative western blot and (D) densitometric quantification of Bcl-xl, Bcl-2, cleaved RAPR-1, cleaved caspase 3, cleaved caspase 9, Bax and Cytc expression in cytosolic and mitochondria. (E) Representative flow cytometry pictures and (F) quantitative analysis of MMP collapse loading with 2.5 mM JC-1. (G) Representative confocal microscopic images of mitochondrial ROS expression. Scale bars, 10 μm. One-way ANOVA and Newman-Keuls multiple comparisons test (B, D, F). $^{*}P < 0.05$, $^{**}P < 0.01$, compared with LG group; $^{\#}P < 0.05$, $^{\#\#}P < 0.01$, compared with HG group.

tiple comparisons test was used for statistical comparisons among experimental groups. Statistical significance was considered with a value of $P < 0.05$.

Results

HQD mitigates HG-induced injury in mouse podocytes

As shown in **Figure 1A**, we determined HQD between 10 to 1000 μg/ml as an appropriate concentration range to have no cytotoxicity on podocyte proliferation. Apocynin, an NADPH oxidase inhibitor, was introduced as positive control. Flow cytometry analysis showed that HG induced significant podocyte apoptosis, while HQD or apocynin protected against HG-induced podocyte apoptosis in a dose-dependent manner (**Figure 1B**, **1C**). The parallel results also concluded from western blot and immunofluorescence staining for Nephrin, a representative marker for podocyte foot process, which further demonstrated that HQD could exert beneficial effect in inhibiting HG-induced podocyte apoptosis (**Figure 1D**, **1E**).

HQD inhibited HG-induced ROS production and oxidative stress in podocytes

Previous studies confirmed that oxidative stress is associated with podocyte apoptosis [25]. Thus, NADPH oxidase activity and ROS production were analyzed. As expected in **Figure 2**, HG significantly enhanced the NADPH oxidase activity and ROS production, and the effect was eliminated by HQD treatment in a dose-dependent manner. Especially, HQD at 300 μg/ml and 1000 μg/ml exerted significant protective effect on HG-triggered apoptosis in podocytes.

As shown in **Figure 3A**, qRT-PCR was used to monitor the expression levels of NADPH oxidase subunits including Nox4, gp91phox, p47phox, p22phox and rac-1. And the results demonstrated Nox4, gp91phox and rac-1 mRNA increased in HG-incubated podocytes, while HQD treatment restored the expression (**Figure 3A**). Additionally, western blot analysis revealed the high expression of Nox4, gp91phox and rac-1 in HG-treated podocytes and the adverse effect of HQD treatment (**Figure 3B**, **3C**). Same trend was observed in immunofluorescence staining which presented the Nox4 expression (**Figure 3D**).

HQD suppressed Nox4/p53/Bax signaling and mitochondria-mediated apoptotic pathway in HG-treated podocytes

Previous trials showed that HG inactivated AMPK, up-regulated Nox4-dependent activation of p53, and induced podocyte apoptosis [11]. Here we revealed that HQD significantly down-regulated HG triggered nuclear expression of p53 and p-p53 (**Figure 4A**, **4B**). The mitochondrial apoptotic pathway is initiated by activation of Bax to the outer mitochondrial membrane, where it accumulates and penetrates the inner mitochondrial membrane and results in Cytc efflux into the cytosol and caspase activation [26, 27]. Consistently, western blot analysis showed that HQD can significant decrease HG-induced Bax expression in mitochondria and Cytc expression in cytosol (**Figure 4C**, **4D**). And HG treatment elevated Bcl-2, Bcl-xl, cleaved RAPR-1, cleaved caspase 9 and caspase 3 expression while HQD dampened the tendency significantly (**Figure 4C**, **4D**). We also found that mitochondrial dysfunction characterized by MMP collapse and ROS production were inhibited with HQD treatment (**Figure 4E-G**).

HQD attenuated HG-induced podocyte apoptosis by regulating Nox4 and p53 expression

To further confirm the role of Nox4 and p53 in mediating the effect of HQD on podocyte apoptosis, exogenous Nox4 and p53 overexpression plasmids were transfected respectively. Western blot analysis showed that Nox4 expression was increased nearly double after Nox4 overexpression plasmid transfection in LG condition (**Figure 5A**, **5B**). As shown in **Figure 5C**, **5D**, the inhibitory effect of HQD on HG-induced podocyte apoptosis was counteracted in Nox4 overexpression podocyte. And the down-regulated

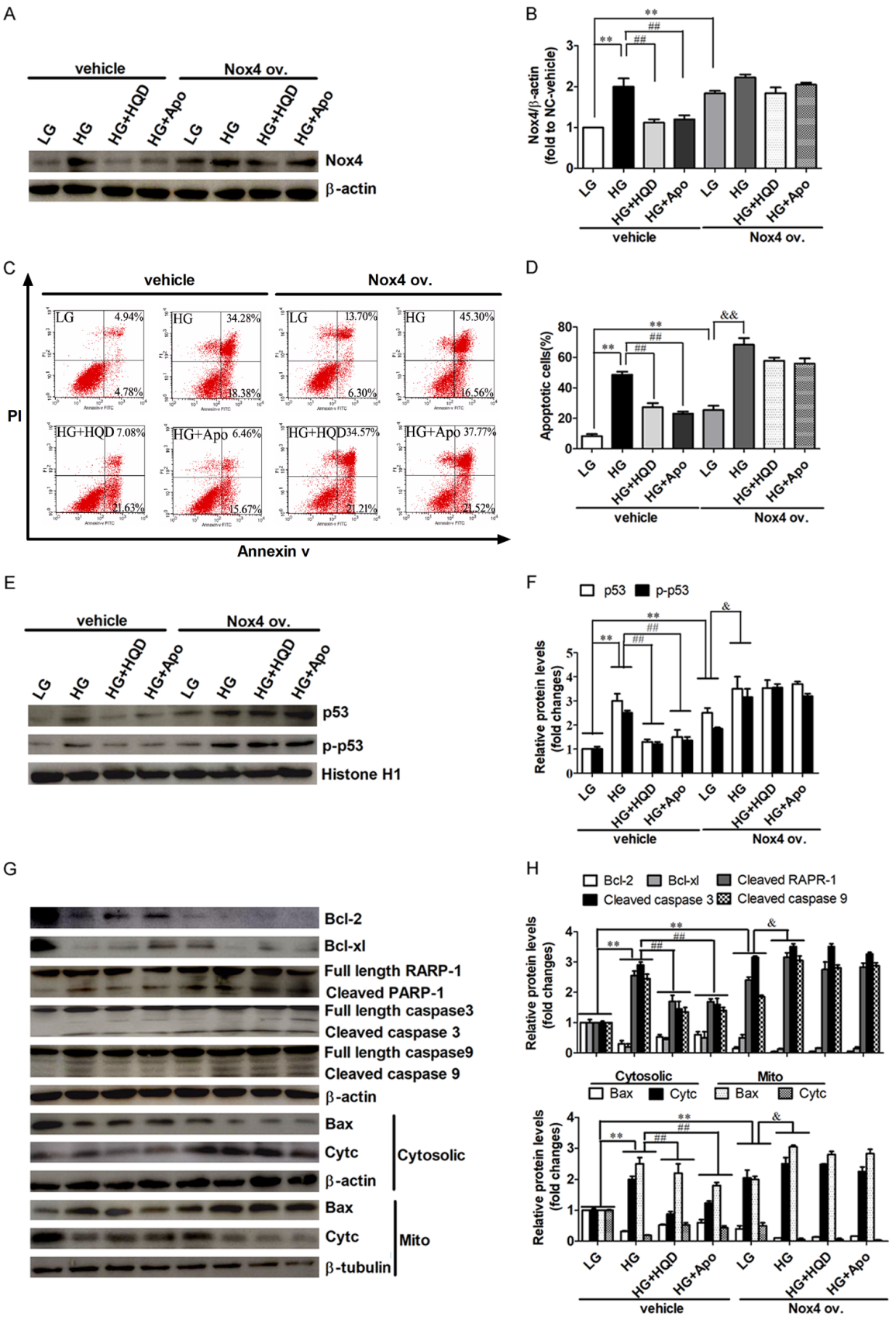
A
vehicle
Nox4 ov.
LG
HG
HG+HQD
HG+Apo
Nox4
β-actin
B
Nox4/β-actin (fold to NC-vehicle)
C
PI
Annexin v
4.94%
4.78%
34.28%
18.38%
13.70%
6.30%
45.30%
16.56%
HG+HQD 7.08%
21.63%
HG+Apo 6.46%
15.67%
HG+HQD34.57%
21.21%
HG+Apo 37.77%
21.52%
D
Apoptotic cells(%)
E
p53
p-p53
Histone H1
F
p53
p-p53
Relative protein levels (fold changes)
G
Bcl-2
Bcl-xl
Full length RARP-1
Cleaved PARP-1
Full length caspase3
Cleaved caspase 3
Full length caspase9
Cleaved caspase 9
β-actin
Bax
Cytc
β-actin
Cytosolic
Bax
Cytc
β-tubulin
Mito
H
Bcl-2
Bcl-xl
Cleaved RAPR-1
Cleaved caspase 3
Cleaved caspase 9
Relative protein levels (fold changes)
Cytosolic
Mito
Bax
Cytc

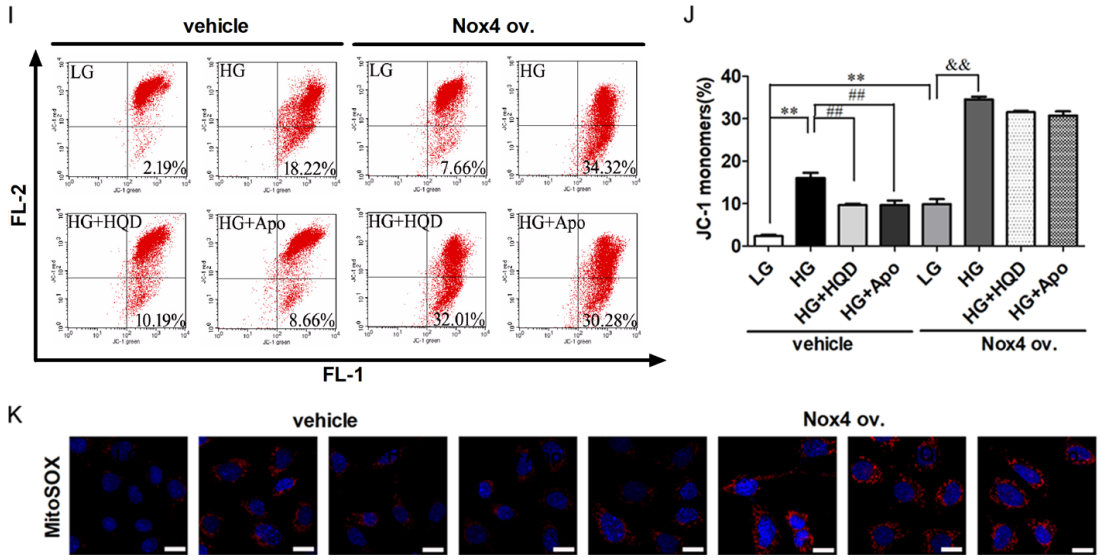

Figure 5. Effect of Nox4 in mediating HQD efficacy on podocyte apoptosis and Nox4/p53/Bax signaling pathway. (A-K) Podocytes were transfected with empty vector (vehicle) or Nox4 overexpression (ov.) plasmid for 24 hours, then treated with HG in the presence or absence of HQD (300 μg/ml) for 72 hours. (A) Western blot and (B) densitometric quantification of Nox4 expression in podocytes transfected with vehicle or Nox4 ov. plasmid. (C) Representative flow cytometry images and (D) quantitative analysis of apoptotic cells. (E) Representative western blot and (F) densitometric quantification of p53 and p-p53 expression. (G) Western blot and (H) densitometric quantification of Bcl-xl, Bcl-2, cleaved RAPR-1, cleaved caspase 3, cleaved caspase 9, Bax and Cytc expression in cytosolic and mitochondria. (I) Representative flow cytometry pictures and (J) quantitative analysis of MMP collapse loading with JC-1. (K) Representative confocal microscopic images of mitochondrial ROS expression. Scale bars, 10 μm. One-way ANOVA and Newman-Keuls multiple comparisons test (B, D, H, J). Unpaired two-tailed t test and Newman-Keuls multiple comparisons test (F). $^{**}P < 0.01$, compared with LG-vehicle group; $^{\#\#}P < 0.01$, compared with HG-vehicle group; $^{\&}P < 0.05$, $^{\&\&}P < 0.01$, compared with LG-Nox4 ov. group.

effect of HQD on the nuclear expression of p53 and p-p53, Nox4/p53/Bax signaling, mitochondria-mediated apoptotic pathway, MMP and ROS production were also abolished in Nox4 overexpression cell (**Figure 5E-K**).

Similarly, western blot analysis presented p53 and p-p53 expression were significantly increased after p53 overexpression plasmid transfection in LG condition (**Figure 6A**, **6B**). p53 overexpression blocked the beneficial effect of HQD on podocyte apoptosis. And the changes which HQD exerted on Nox4/p53/Bax signaling, mitochondria-mediated apoptotic pathway, MMP and ROS production were eliminated as same as Nox4 overexpression (**Figure 6C-I**). Intriguingly, p53 overexpression did not alter the expression of Nox4, which suggest that Nox4 is the upstream signaling of p53 (**Figure 6E**, **6F**).

HQD prevented the development of DN and podocyte apoptosis in STZ-induced diabetic mice

As expected, compared with the NC-vehicle, urinary albumin to creatinine ratio (ACR) was markedly increased in DN-vehicle mice at 2nd week after a two-dose STZ injection. Addition of HQD significant prevented the development of albuminuria at 10th week (**Figure 7A**). Consistently, blood urea nitrogen (BUN) levels were significant reduced with HQD treatment while without altering the serum creatinine level (**Figure 7B**, **7C**).

PAS staining showed that DN mice exhibited increased glomerular surface area, expanded mesangial matrix and severe glomerulosclerosis compared with NC-vehicle group. In contrast, HQD treatment markedly attenuated those abnormal changes (**Figure 7D**, **7E**).

Western blot analyses revealed that podocyte foot process markers Nephrin and podocyte nucleus marker Wilms tumor 1 (WT1) were significant downregulated in DN-vehicle mice, which indicate the glomerular filtration barrier was injured. However, HQD restored the expression of Nephrin and WT1 in diabetic kidney, which similar with the efficacy of apocynin (**Figure 7F**, **7G**).

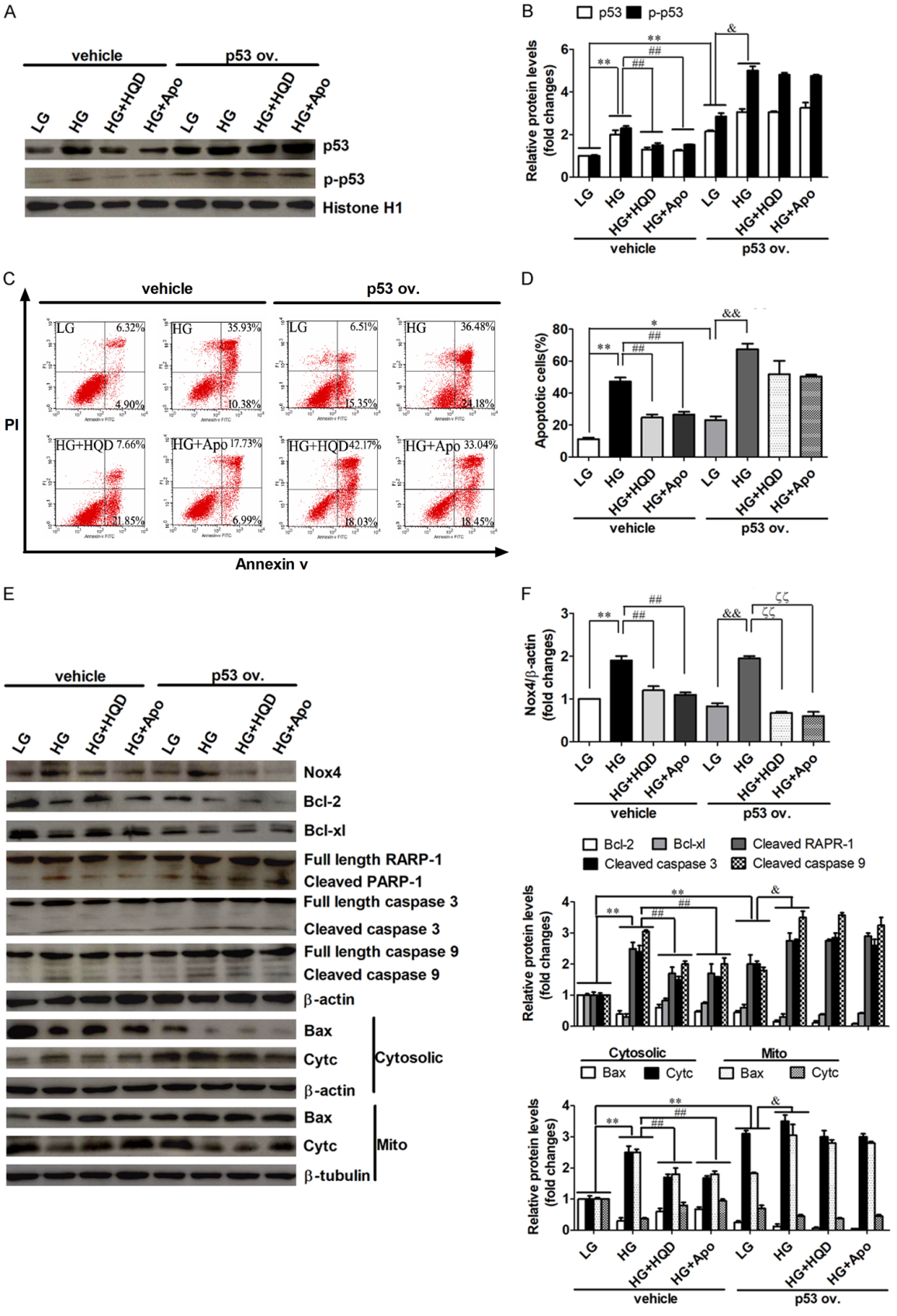
A
vehicle
p53 ov.
LG
HG
HG+HQD
HG+Apo
p53
p-p53
Histone H1
B
p53
p-p53
Relative protein levels (fold changes)
C
PI
Annexin v
LG 6.32% 4.90%
HG 35.93% 10.38%
LG 6.51% 15.35%
HG 36.48% 24.18%
HG+HQD 7.66% 21.85%
HG+Apo 17.73% 6.99%
HG+HQD 42.17% 18.03%
HG+Apo 33.04% 18.45%
D
Apoptotic cells(%)
E
Nox4
Bcl-2
Bcl-xl
Full length RARP-1
Cleaved PARP-1
Full length caspase 3
Cleaved caspase 3
Full length caspase 9
Cleaved caspase 9
β-actin
Bax
Cytc
Cytosolic
β-actin
Bax
Cytc
Mito
β-tubulin
F
Nox4/β-actin (fold changes)
Bcl-2
Bcl-xl
Cleaved RAPR-1
Cleaved caspase 3
Cleaved caspase 9
Cytosolic
Mito
Bax
Cytc

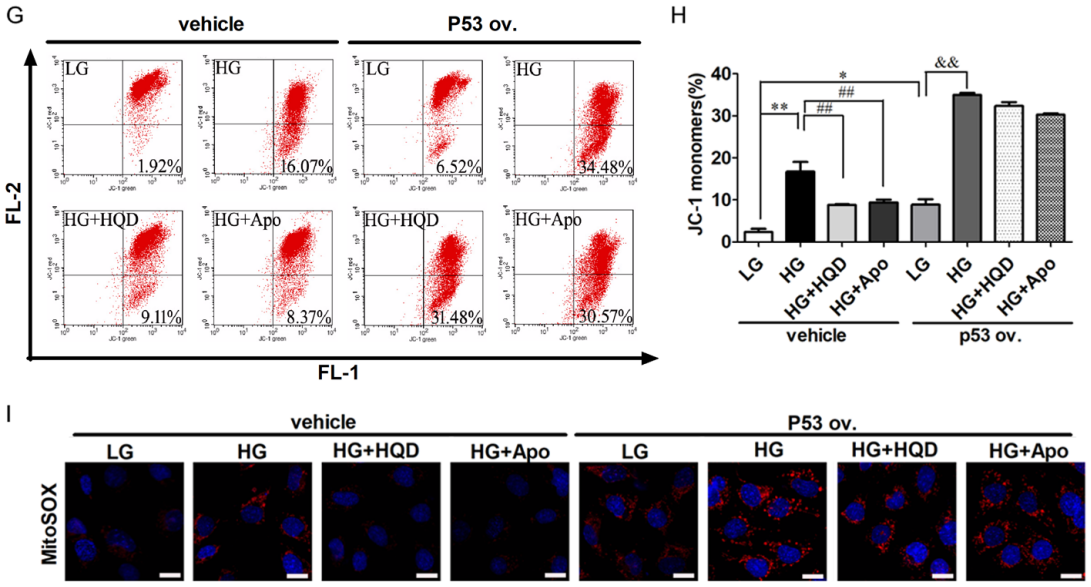

Figure 6. Effect of p53 in mediating HQD efficacy on podocyte apoptosis and Nox4/p53/Bax signaling pathway. (A-I) Podocytes were transfected with vehicle and p53 ov. plasmid for 24 hours, then treated with HG in the presence or absence of HQD (300 μg/ml) for 72 hours. (A) Western blot and (B) densitometric quantification of the nuclear p53 and p-p53 expression in podocytes transfected with vehicle or p53 ov. plasmid. (C) Representative flow cytometry images and (D) quantitative analysis of apoptotic cells. (E) Western blot and (F) densitometric quantification of Nox4, Bcl-xl, Bcl-2, cleaved RAPR-1, cleaved caspase 3, cleaved caspase 9, Bax and Cytc expression in cytosolic and mitochondria. (G) Representative flow cytometry pictures and (H) quantitative analysis of MMP collapse loading with JC-1. (I) Representative confocal microscopic images of mitochondrial ROS expression. Scale bars, 10 μm. One-way ANOVA and Newman-Keuls multiple comparisons test (B, D, F, H). $^{*}P < 0.05$, $^{**}P < 0.01$, compared with LG-vehicle group; $^{\#\#}P < 0.01$, compared with HG-vehicle group; $^{\&}P < 0.05$, $^{\&\&}P < 0.01$, compared with LG-p53 ov. group; $^{\zeta\zeta}P < 0.01$, compared with HG-p53 ov. group.

HQD inhibited oxidative stress and Nox4/p53/Bax signaling pathway in the kidney of STZ-induced diabetic mice

Next, the effect of HQD on oxidative stress and Nox4/p53/Bax signaling pathway in the kidney of STZ-induced diabetic mice were investigated. Western blot analyses showed that the expression levels of Nox4, gp91phox and rac-1 was dramatically up-regulated in DN-vehicle group compared with NC-vehicle group, while HQD treatment rescued the tendency (**Figure 8A-D**). Immunohistochemistry staining for Nox4 further confirmed the repression of HQD on diabetes-induced oxidative stress (**Figure 8E**).

As shown in **Figure 9A**, **9B**, compared with NC-vehicle mice, the protein levels of p53 and p-p53 in DN-vehicle mice increased significantly and HQD decreased the expression. Likewise, diabetes-induced activation of Nox4/p53/Bax signaling pathway transducers, including Bcl-2, Bcl-xl, Bax, cleaved RAPR-1, cleaved caspase 9 and caspase 3 were significantly attenuated with HQD treatment (**Figure 9C**, **9D**).

Discussion

In this study, we report that HQD exhibited a prominent renoprotection in HG or hyperglycemia-induced podocyte apoptosis, as evidenced by increased the expression of podocyte markers *in vitro* and *in vivo*. And the protective effect of HQD was mediated at least partly by down-regulating Nox4/p53/Bax signaling, which was associated with oxidative stress and mitochondrial dysfunction. These results may highlight HQD as an antiproteinuric drug targeting podocyte for DN therapy.

DN is a long-term complication of diabetes that develops in about 30% of patients with type 1 diabetes, with pathological hallmarks of proteinuria and glomerulosclerosis [28]. Podocytes cover the exterior basement membrane surface of the glomerular capillary and maintain the structural integrity of glomerular capillary loops and podocytes apoptosis plays a key role in the pathogenesis of DN [29]. Here, we obtained similar result that HQD exhibited inhibitory efficacy on podocyte apoptosis both

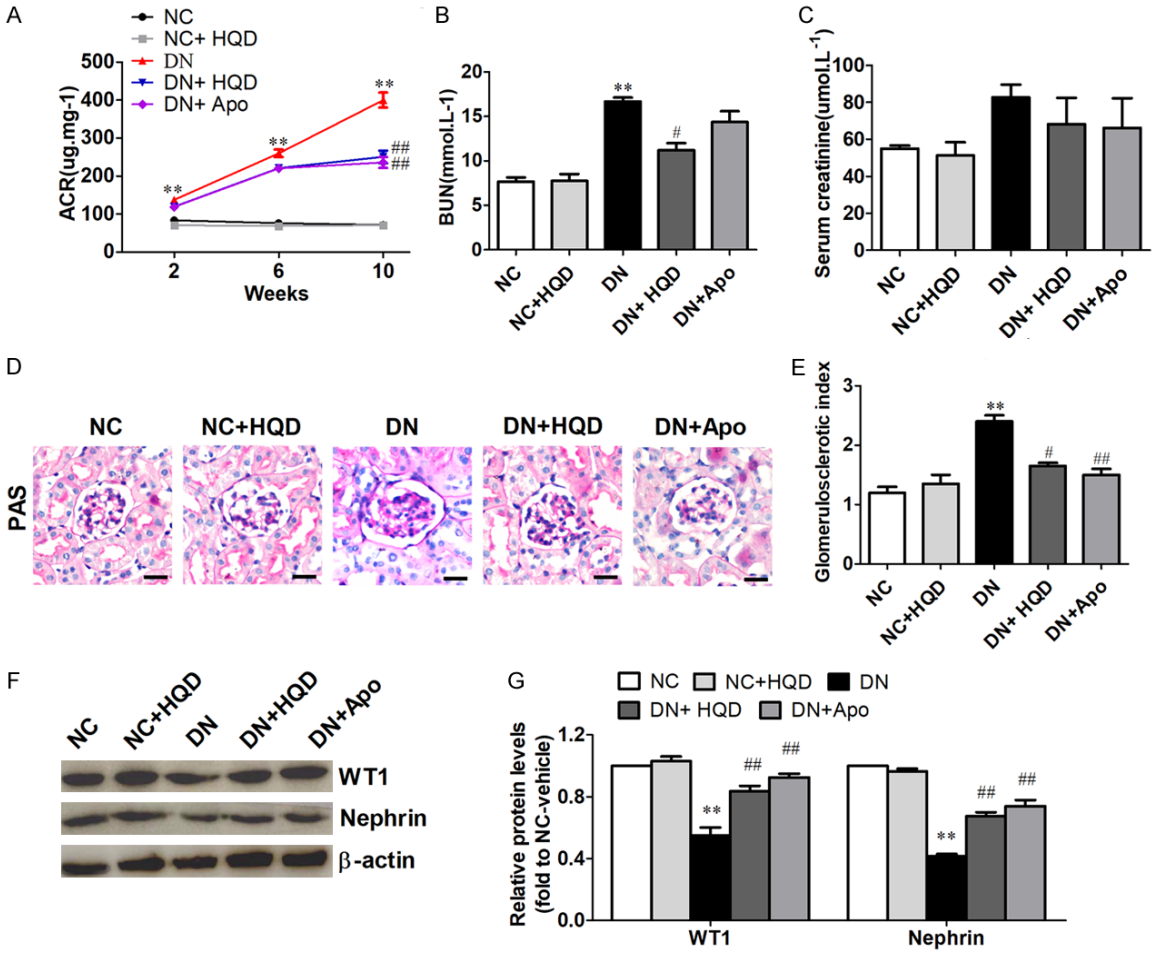

Figure 7. HQD prevented the development of DN in STZ-induced diabetic mice. (A) ACR was measured at 4-week intervals. (B) Serum BUN and (C) serum creatinine were detected at the end of the study. (D) PAS staining. Scale bars, 10 μm. (E) Glomerulosclerotic index based on PAS staining. (F) Representative western blot and (G) densitometric quantification of WT-1 and Nephrin expression in total lysates of kidney cortex from each group. One-way ANOVA and Newman-Keuls multiple comparisons test (A-C, E). Unpaired two-tailed t test and Newman-Keuls multiple comparisons test (G). $^{**}P < 0.01$, compared with normal control (NC) group; $^{\#}P < 0.05$, $^{\#\#}P < 0.01$, compared with the diabetic nephropathy (DN) group (n=8).

in HG-induced podocyte and in STZ-treated mice, which indicate the protective effect of HQD on podocytes. Besides, HQD treatment markedly attenuated albuminuria, reduced serum BUN and ameliorated glomerular histopathology in STZ-induced diabetic mice, suggesting HQD can effectively prevent the progression of DN. Consistent with our previous investigation, it is worth noting that there was no significant difference in serum creatinine between the NC group and the DN group, which indicate serum creatinine may not be a sensitive indicator for renal dysfunction [30].

NADPH oxidases, the major sources of ROS generation, play essential role in mediating oxidative stress and promoting podocyte injury in diabetes [31]. Previous studies found that HG incubation increased NADPH oxidase isoforms Nox4 and Nox1 mRNA and protein expression [6]. Nox4 deficiency reduced podocyte apoptosis significantly in diabetic milieu [10]. And in diabetic Nox1-/-ApoE-/-mice, albuminuria level is unaffected but significantly decreased in diabetic Nox4-/-ApoE-/-mice when compared to diabetic wild-type control [32]. Consistent with those investigations, our present results proved Nox4 is indeed up-regulated in hyperglycemia. Nox4 overexpression dramatically triggered oxidative stress and inhibited the protective effect of HQD on HG-induced apoptosis, indicating that Nox4 mediated the inhibitory effect of HQD

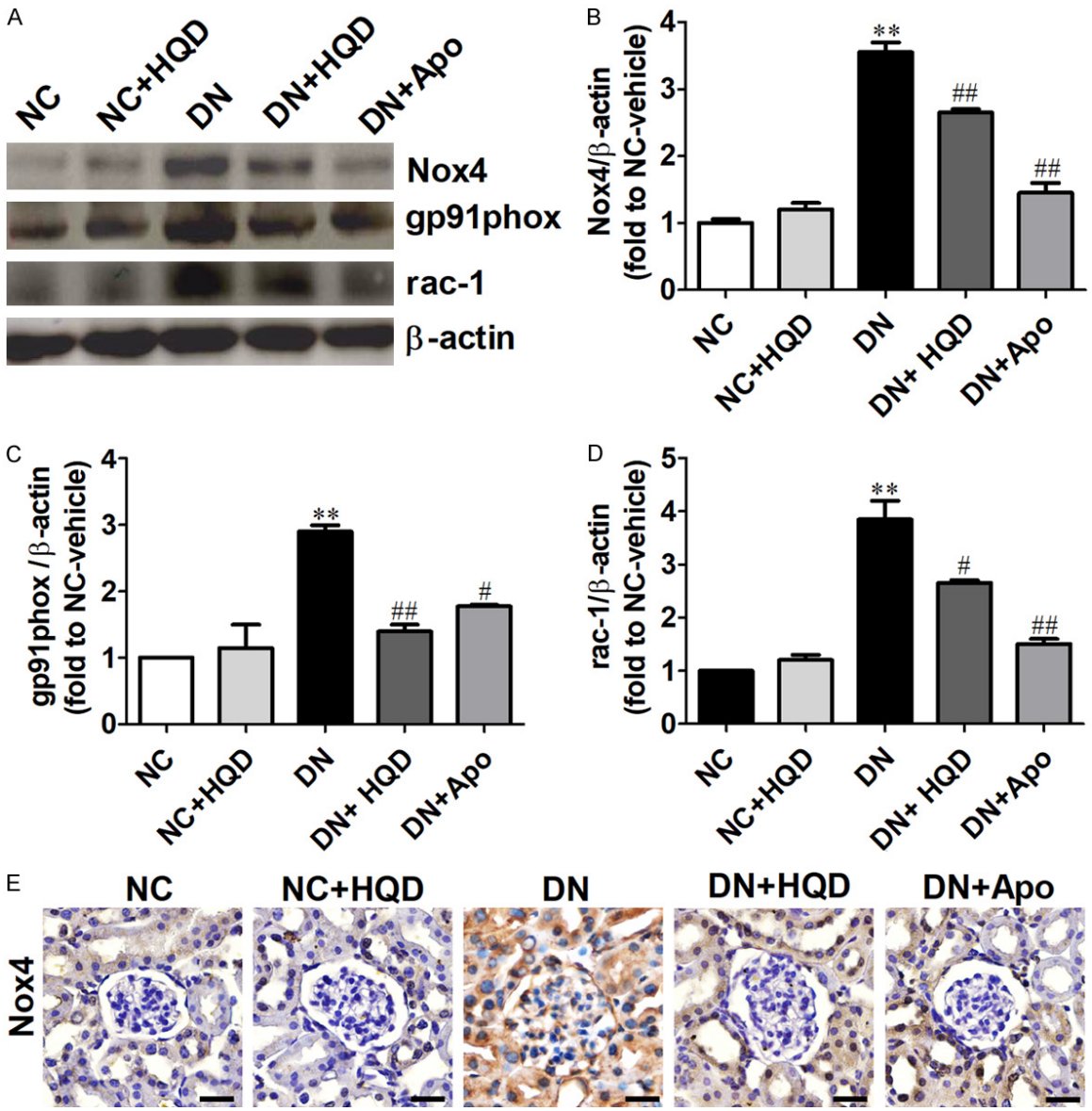

Figure 8. Effect of HQD on Nox4, gp91phox and rac-1 protein expression in the kidney of STZ-induced diabetic mice. (A) Western blot and (B-D) densitometric quantification of Nox4, gp91phox and rac-1 expression. (E) Representative immunohistochemistry staining for Nox4 expression. Scale bars, 10 μm. One-way ANOVA and Newman-Keuls multiple comparisons test (B-D). $^{**}P < 0.01$, compared with NC group; $^{\#}P < 0.05$, $^{\#\#}P < 0.01$, compared with DN group (n=8).

on HG-induced oxidative stress. Collectively, these data strongly suggest that HQD can protect diabetes/HG-inflicted podocyte apoptosis at least in part via inhibiting oxidative stress involving down-regulation of Nox4 expression.

Nox4 induces podocyte injure by activating its downstream signaling pathway, in which p53 are included [11, 33]. p53 is a well-known tumor suppressor and is also involved in processes of apoptosis [34]. Coincidentally, our research suggested that p53 overexpression had no obvious impact on Nox4 expression, indicating p53 indeed acted as the downstream of Nox4. Furthermore, our data showed that both p53 and p-p53 expression were significantly increased in HG-incubated mouse podocytes and renal cortex of DN mice, while were significantly reduced by HQD. Accordingly, p53 overexpression prevented the protective effect

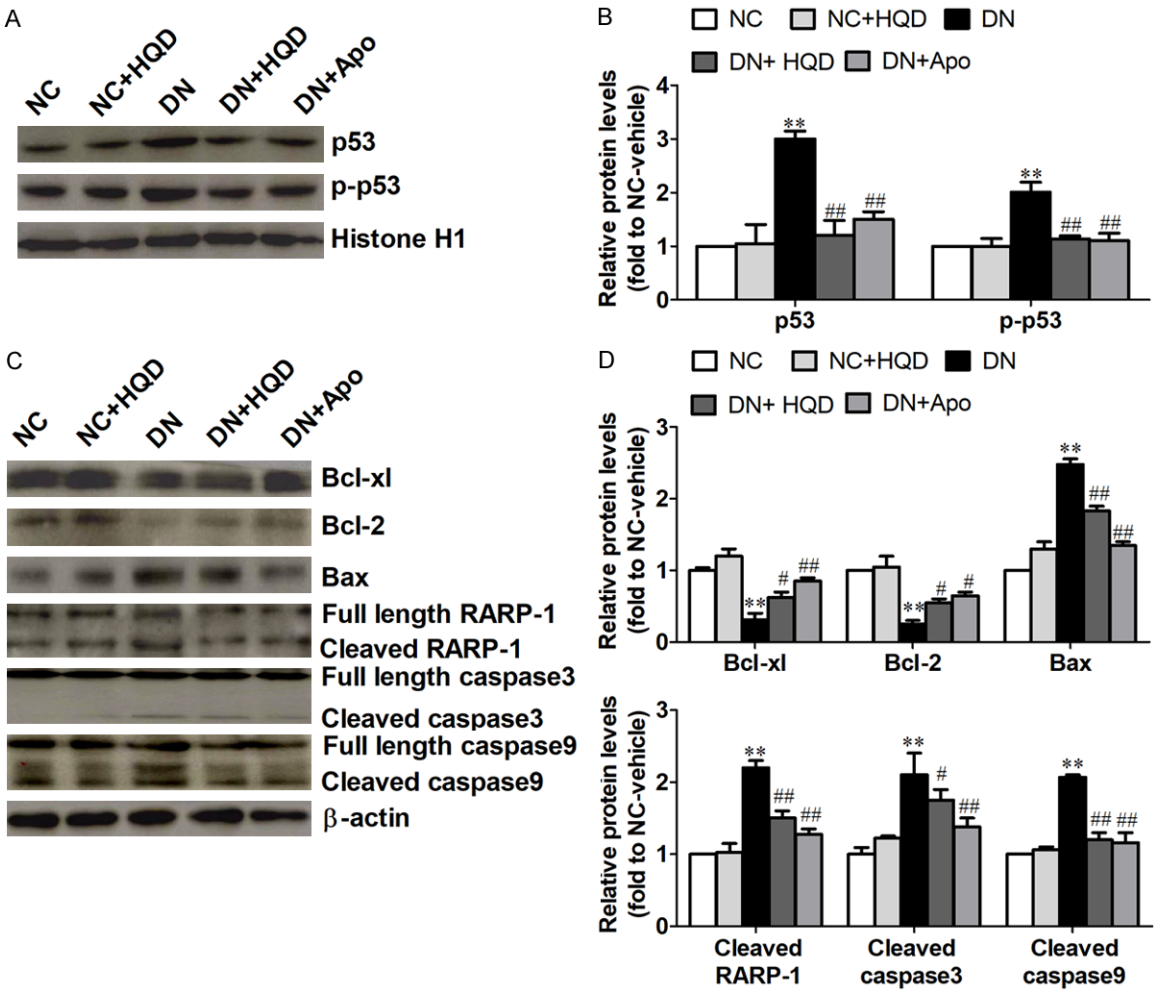

Figure 9. Effect of HQD on mitochondrial-mediated apoptotic pathway in the kidney of STZ-induced diabetic mice. (A) Western blot and (B) densitometric quantification of p53 and p-p53 expression. (C) Western blot and (D) densitometric quantification of Bcl-xl, Bcl-2, Bax, cleaved RAPR-1, cleaved caspase 3 and cleaved caspase 9 expression. One-way ANOVA and Newman-Keuls multiple comparisons test (B, D). $^{**}P < 0.01$, compared with NC group; $^{\#}P < 0.05$, $^{\#\#}P < 0.01$, compared with DN group (n=8).

of HQD on HG-induced podocyte apoptosis, indicating p53 involved in mediating the inhibitory effect of HQD to HG-induced damage.

Previous study reported that p53 can directly activate the pro-apoptotic protein Bax in initiating apoptosis through mitochondrial pathway [35, 36], which largely contribute to the development of DN [37, 38]. The mitochondrial cell death pathway results from dysfunctional mitochondria, which exhibit fragmentation and membrane depolarization, massive amounts of ROS generation and apoptogenic proteins (e.g., caspase-3) release in response to stressors. As expected, our study revealed an enhanced activity of mitochondria-mediated apoptotic pathway in HG-treated podocytes and DN mice, which were significantly reversed by HQD treatment. Nox4 and p53 overexpression can activate the pathway while the inhibitory efficacy of HQD on the pathway were negative regulated, which suggest up-regulation of Nox4 and p53 involved in activating the mitochondria-mediated apoptotic pathway and HQD may exhibit efficacy through this pathway. In other words, Nox4 and p53 may be the intervention target of HQD to ameliorate podocyte apoptosis and more details need to be studied in the future.

Conclusion

In summary, this study reveals that HQD possesses efficacy to impede HG/hyperglycemia-induced podocyte apoptosis, and the mecha-

nism may correlate with inhibiting oxidative stress which mediated by Nox4/p53/Bax signaling. Considering the improvement of HQD on restoring renal functional and histological injury, we propose that HQD may be a beneficial therapeutic strategy for DN.

Acknowledgements

This study was supported by the Key Medical Discipline Project of Shanghai Municipal Health Bureau (ZK2015A18), Independent Innovation Research Fund of Putuo District Science and Technology Committee (2012PTKW006) and the Innovation Program of Talent Project of Putuo District (2016202A).

Disclosure of conflict of interest

None.

Address correspondence to: Wen Peng, Department of Nephrology, Laboratory of Renal Disease, Putuo Hospital, Shanghai University of Traditional Chinese Medicine, 164 Lanxi Road, Shanghai 200062, China. Fax: +86-21-52665957; E-mail: pengwen_01@vip.sina.com; Li Wang, Laboratory of Renal Disease, Putuo Hospital, Shanghai University of Traditional Chinese Medicine, 164 Lanxi Road, Shanghai 200062, China. Fax: +86-21-52669731; E-mail: wanglitcm2007@163.com

References

[1] Xue R, Gui D, Zheng L, Zhai R, Wang F and Wang N. Mechanistic insight and management of diabetic nephropathy: recent progress and future perspective. J Diabetes Res 2017; 2017: 1839809.

[2] Ilyas Z, Chaiban JT and Krikorian A. Novel insights into the pathophysiology and clinical aspects of diabetic nephropathy. Rev Endocr Metab Disord 2017; 18: 21-28.

[3] Brosius FC and Coward RJ. Podocytes, signaling pathways, and vascular factors in diabetic kidney disease. Adv Chronic Kidney Dis 2014; 21: 304-310.

[4] Gnudi L, Coward RJM and Long DA. Diabetic nephropathy: perspective on novel molecular mechanisms. Trends Endocrinol Metab 2016; 27: 820-830.

[5] Wang B, Xu X, He X, Wang Z and Yang M. Berberine improved aldo-induced podocyte injury via inhibiting oxidative stress and endoplasmic reticulum stress pathways both in vivo and in vitro. Cell Physiol Biochem 2016; 39: 217-228.

[6] Eid S, Boutary S, Braych K, Sabra R, Massaad C, Hamdy A, Rashid A, Moodad S, Block K, Gorin Y, Abboud HE and Eid AA. mTORC2 signaling regulates nox4-induced podocyte depletion in diabetes. Antioxid Redox Signal 2016; 25: 703-719.

[7] Al-Harbi NO, Nadeem A, Ansari MA, Al-Harbi MM, Alotaibi MR, AlSaad AM and Ahmad SF. Psoriasis-like inflammation leads to renal dysfunction via upregulation of NADPH oxidases and inducible nitric oxide synthase. Int Immunopharmacol 2017; 46: 1-8.

[8] Gorin Y, Cavaglieri RC, Khazim K, Lee DY, Bruno F, Thakur S, Fanti P, Szyndralewiez C, Barnes JL, Block K and Abboud HE. Targeting NADPH oxidase with a novel dual Nox1/Nox4 inhibitor attenuates renal pathology in type 1 diabetes. Am J Physiol Renal Physiol 2015; 308: F1276-1287.

[9] Eid AA, Lee DY, Roman LJ, Khazim K and Gorin Y. Sestrin 2 and AMPK connect hyperglycemia to Nox4-dependent endothelial nitric oxide synthase uncoupling and matrix protein expression. Mol Cell Biol 2013; 33: 3439-3460.

[10] Eid AA, Ford BM, Bhandary B, de Cassia CR, Block K, Barnes JL, Gorin Y, Choudhury GG and Abboud HE. Mammalian target of rapamycin regulates Nox4-mediated podocyte depletion in diabetic renal injury. Diabetes 2013; 62: 2935-2947.

[11] Eid AA, Ford BM, Block K, Kasinath BS, Gorin Y, Ghosh-Choudhury G, Barnes JL and Abboud HE. AMP-activated protein kinase (AMPK) negatively regulates Nox4-dependent activation of p53 and epithelial cell apoptosis in diabetes. J Biol Chem 2010; 285: 37503-37512.

[12] Muscella A, Vetrugno C, Cossa LG, Antonaci G, Barca A, De Pascali SA, Fanizzi FP and Marsigliante S. Apoptosis by [Pt(O,O'-acac)(gamma-acac)(DMS)] requires PKC-delta mediated p53 activation in malignant pleural mesothelioma. PLoS One 2017; 12: e0181114.

[13] Li C, Jeong Y and Kim M. Mammea longifolia planch. and triana fruit extract induces cell death in the human colon cancer cell line, SW-480, via mitochondria-related apoptosis and activation of p53. J Med Food 2017; 20: 485-490.

[14] Prenek L, Boldizsar F, Kugyelka R, Ugor E, Berta G, Nemeth P and Berki T. The regulation of the mitochondrial apoptotic pathway by glucocorticoid receptor in collaboration with Bcl-2 family proteins in developing T cells. Apoptosis 2017; 22: 239-253.

[15] Cong H, Du N, Yang Y, Song L, Zhang W and Tien P. Enterovirus 71 2B induces cell apoptosis by directly inducing the conformational activation of the proapoptotic protein bax. J Virol 2016; 90: 9862-9877.

[16] Jiang MQ, Wang L, Cao AL, Zhao J, Chen X, Wang YM, Wang H and Peng W. Huangqi decoction improves renal tubulointerstitial fibrosis in mice by inhibiting the up-regulation of Wnt/beta-catenin signaling pathway. Cell Physiol Biochem 2015; 36: 655-669.

[17] Zhao J, Wang L, Cao AL, Jiang MQ, Chen X, Wang Y, Wang YM, Wang H, Zhang XM and Peng W. Huangqi decoction ameliorates renal fibrosis via TGF-β/Smad signaling pathway in vivo and in vitro. Cell Physiol Biochem 2016; 38: 1761-1774.

[18] Han H, Cao A, Wang L, Guo H, Zang Y, Li Z, Zhang X and Peng W. Huangqi decoction ameliorates streptozotocin-induced rat diabetic nephropathy through antioxidant and regulation of the TGF-beta/MAPK/PPAR-gamma signaling. Cell Physiol Biochem 2017; 42: 1934-1944.

[19] Guo H, Cao A, Chu S, Wang Y, Zang Y, Mao X, Wang H, Wang Y, Liu C, Zhang X and Peng W. Astragaloside IV attenuates podocyte apoptosis mediated by endoplasmic reticulum stress through upregulating sarco/endoplasmic reticulum Ca2+-ATPase 2 expression in diabetic nephropathy. Front Pharmacol 2016; 7: 500.

[20] Guo H, Wang Y, Zhang X, Zang Y, Zhang Y, Wang L, Wang H, Wang Y, Cao A and Peng W. Astragaloside IV protects against podocyte injury via SERCA2-dependent ER stress reduction and AMPKα-regulated autophagy induction in streptozotocin-induced diabetic nephropathy. Sci Rep 2017; 7: 6852.

[21] Chu S, Mao XD, Wang L and Peng W. Effects of Huang Qi decoction on endothelial dysfunction induced by homocysteine. Evid Based Complement Alternat Med 2016; 2016: 7272694.

[22] Sakellariou GK, Vasilaki A, Palomero J, Kayani A, Zibrik L, McArdle A and Jackson MJ. Studies of mitochondrial and nonmitochondrial sources implicate nicotinamide adenine dinucleotide phosphate oxidase(s) in the increased skeletal muscle superoxide generation that occurs during contractile activity. Antioxid Redox Signal 2013; 18: 603-21.

[23] Yuan Z, Cao A, Liu H, Guo H, Zang Y, Wang Y, Wang H, Yin P and Peng W. Calcium uptake via mitochondrial uniporter contributes to palmitic acid-induced apoptosis in mouse podocytes. J Cell Biochem 2017; 118: 2809-2818.

[24] Zhan M, Usman IM, Sun L and Kanwar YS. Disruption of renal tubular mitochondrial quality control by Myo-inositol oxygenase in diabetic kidney disease. J Am Soc Nephrol 2015; 26: 1304-1321.

[25] Sun LN, Liu XC, Chen XJ, Guan GJ and Liu G. Curcumin attenuates high glucose-induced podocyte apoptosis by regulating functional connections between caveolin-1 phosphorylation and ROS. Acta Pharmacologica Sinica 2016; 37: 645-655.

[26] Edlich F, Banerjee S, Suzuki M, Cleland MM, Arnoult D, Wang C, Neutzner A, Tjandra N and Youle RJ. Bcl-x(L) retrotranslocates Bax from the mitochondria into the cytosol. Cell 2011; 145: 104-116.

[27] Chen HC, Kanai M, Inoue-Yamauchi A, Tu HC, Huang Y, Ren D, Kim H, Takeda S, Reyna DE, Chan PM, Ganesan YT, Liao CP, Gavathiotis E, Hsieh JJ and Cheng EH. An interconnected hierarchical model of cell death regulation by the BCL-2 family. Nat Cell Biol 2015; 17: 1270-1281.

[28] Perkins BA, Ficociello LH, Ostrander BE, Silva KH, Weinberg J, Warram JH and Krolewski AS. Microalbuminuria and the risk for early progressive renal function decline in type 1 diabetes. J Am Soc Nephrol 2007; 18: 1353-1361.

[29] Liu BC, Song X, Lu XY, Li DT, Eaton DC, Shen BZ, Li XQ and Ma HP. High glucose induces podocyte apoptosis by stimulating TRPC6 via elevation of reactive oxygen species. Biochim Biophys Acta 2013; 1833: 1434-1442.

[30] Chen X, Wu R, Kong Y, Yang Y, Gao Y, Sun D, Liu Q, Dai D, Lu Z, Wang N, Ge S and Wang F. Tanshinone IIA attenuates renal damage in STZ-induced diabetic rats via inhibiting oxidative stress and inflammation. Oncotarget 2017; 8: 31915-31922.

[31] Khazim K, Gorin Y, Cavaglieri RC, Abboud HE and Fanti P. The antioxidant silybin prevents high glucose-induced oxidative stress and podocyte injury in vitro and in vivo. AJP: Renal Physiology 2013; 305: F691-F700.

[32] Jha JC, Gray SP, Barit D, Okabe J, El-Osta A, Namikoshi T, Thallas-Bonke V, Wingler K, Szyndralewiez C, Heitz F, Touyz RM, Cooper ME, Schmidt HH and Jandeleit-Dahm KA. Genetic targeting or pharmacologic inhibition of NADPH oxidase nox4 provides renoprotection in long-term diabetic nephropathy. J Am Soc Nephrol 2014; 25: 1237-1254.

[33] Park CH, Shin SH, Lee EK, Kim DH, Kim MJ, Roh SS, Yokozawa T and Chung HY. Magnesium lithospermate B from salvia miltiorrhiza bunge ameliorates aging-induced renal inflammation and senescence via NADPH oxidase-mediated reactive oxygen generation. Phytother Res 2017; 31: 721-728.

[34] Yuan Y, Zhang A, Qi J, Wang H, Liu X, Zhao M, Duan S, Huang Z, Zhang C, Wu L, Zhang B and Xing C. P53/Drp1-dependent mitochondrial fission mediates aldosterone-induced podocyte injury and mitochondrial dysfunction. Am J Physiol Renal Physiol 2017; 314: 798-808.

[35] Banerjee S and Chaturvedi CM. Apoptotic mechanism behind the testicular atrophy in photorefractory and scotosensitive quail: Involve-

ment of GnIH induced p-53 dependent Bax-Caspase-3 mediated pathway. J Photochem Photobiol B 2017; 176: 124-135.

[36] Gao M, Huang Y, Wang L, Huang M, Liu F, Liao S, Yu S, Lu Z, Han S, Hu X, Qu Z, Liu X, Assefa YT, Yang L, Tang Z, Li DW and Liu M. HSF4 regulates lens fiber cell differentiation by activating p53 and its downstream regulators. Cell Death Dis 2017; 8: e3082.

[37] Higgins GC and Coughlan MT. Mitochondrial dysfunction and mitophagy: the beginning and end to diabetic nephropathy? Br J Pharmacol 2014; 171: 1917-1942.

[38] Sun L, Dutta RK, Xie P and Kanwar YS. myo-inositol oxygenase overexpression accentuates generation of reactive oxygen species and exacerbates cellular injury following high glucose ambience: a new mechanism relevant to the pathogenesis of diabetic nephropathy. J Biol Chem 2016; 291: 5688-5707.